Vacuum Systems for Laboratory Gas Phase Spectroscopy

A Major Qualifying Project (MQP) Report submitted to the
faculty of Worcester Polytechnic Institute in partial fulfillment of the requirements
for the Degree of Bachelor of Science in Physics

By:
Valerie Bennett

Project Advisor:
Dr. Douglas Petkie

Date:
May 31, 2024

Abstract

This project is building on previous MQPs focusing on terahertz molecular gas phase spectroscopy for interstellar applications. Previous groups reported having issues with leaks in the vacuum system. This project's goals are to model the system, locate the leak, and determine how to best fix the leak. In modeling the system, we considered the ideal pressure for high-resolution spectroscopy, which we determined to be in the low 10s millitorr region. This project also discusses why the vacuum system is needed, its design and performance, and the problems with having a leak and the absorption cell design.

Acknowledgments

Thank you to my advisor, Professor Douglas Petkie, for your support and guidance throughout this project.

I would like to thank WPI Physics Department's Laboratory for Education and Application Prototypes (LEAP) facility for providing the space and equipment to complete this project.

I would also like to thank Jacob Bouchard and Alex Kiely for their help both in and out of the lab.

Contents

1 Introduction

This project is building on previous MQPs focusing on creating and improving a gas-phase spectrometer. The purpose of this spectrometer is to study terahertz molecular spectroscopy for interstellar applications. Previous groups reported having issues with leaks in the system. This project's goals are to model the system, locate the leak, and determine how to best fix the leak.

In laboratory spectroscopy, being able to study molecules in vacuum is crucial. Depending on the type of spectroscopy and spectral region, different pressures are needed to get the best and most resolute results. Line broadening decreases the resolution of lines, which includes pressure broadening and Doppler broadening. Considering the purpose of spectroscopy for interstellar applications, the conditions of interstellar medium need to be considered. The low density of interstellar medium means the only type of line broadening in space is Doppler broadening, with basically no pressure broadening. For our laboratory spectroscopy, we need to create conditions so that pressure broadening is minimized, and we need to be able to keep the conditions relatively constant.

2 Background

The following sections will be explaining Terahertz spectroscopy for interstellar applications, the need for vacuum systems in spectroscopy, and about vacuum systems in general.

2.1 Spectroscopy for interstellar applications

Spectroscopy is the study of the interaction between electromagnetic radiation and matter. Electromagnetic radiation has an energy $E = h\nu$, dependent on the frequency ν. Upon interacting with an atom or molecule, the energy can be transferred to the atom or molecule, resulting in changes in energy states, called excitation. These energy states can be represented as $E_{initial}$ and E_{final}. For radiation to excite an atom, the energy should be equal to $\Delta E = E_{final} - E_{initial}$. Specific changes in energy states correspond to certain frequencies.

$$h\nu = \Delta E = E_{final} - E_{initial} \qquad \textit{eq 1}$$

If the initial energy is higher than the final energy, electromagnetic radiation is emitted as opposed to absorbed. This is de-excitation, and results in radiation with energy equal to the change in energy states as shown in equation 1 [5]. We can detect the change in energy states using spectroscopy. Specifically, we can measure the frequency of radiation either absorbed or emitted. In the terahertz region, this radiation is due to changes in the rotational energy levels of the molecules of interest. This creates unique spectra that can be used to identify molecules in the interstellar medium.

It is hard to study bodies in space directly because of the extreme conditions and distance. The best way to study these bodies from earth is using spectroscopy. An object's spectrum can be studied to determine makeup, temperature, density, and other characteristics. To be able to detect certain molecules in space, a reference spectrum is needed. This is done with laboratory absorption spectroscopy.

2.2 Spectroscopy vacuum systems

2.2.1 Lines and line shapes

Spectra are groups of lines representing the frequencies detected. Each line represents a specific energy state change and is labeled by the frequency or wavelength produced by the change. Each element has its own unique spectrum, as shown in figure 1.

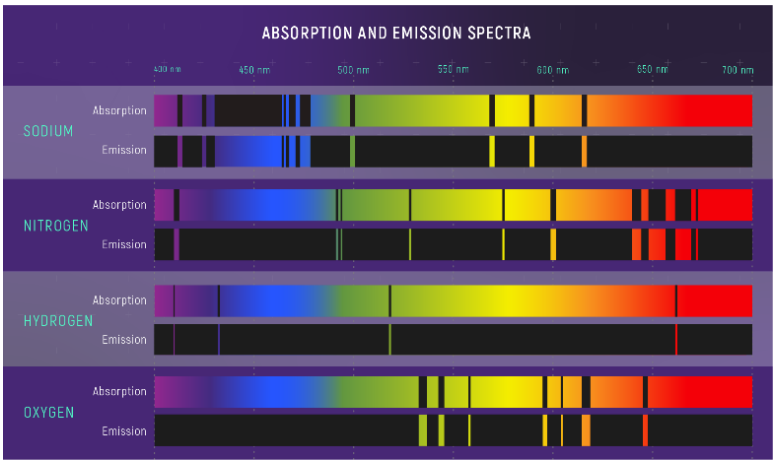

Figure 1: Examples of atomic absorption and emission spectra [1].

The graph of a single line's intensity versus frequency is a curve, as seen in figure 2. This is the line shape. These can be either homogeneous or inhomogeneous. Homogeneous line shapes are when each molecule has identical spectra. This is often seen when the sample, the molecule we want to study, is in the gas phase, as in our case. Inhomogeneous line shapes are when each molecule has different spectra. This is seen when the sample is dissolved in liquid or is in liquid phase [8].

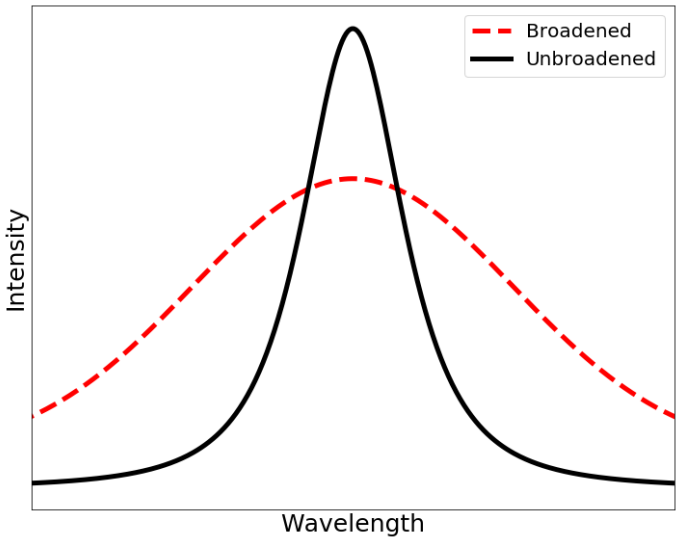

Figure 2: Graph of a spectral line both unbroadened (natural linewidth) and broadened [7].

Each line has a certain natural linewidth intrinsic to the atom or molecule. This is due to the Heisenberg Uncertainty Principle, which relates the lifetime of a state, Δt, and the uncertainty in energy, ΔE.

$$\Delta t * \Delta E \geq \frac{\hbar}{2} \qquad \textit{eq 2}$$

Energy uncertainty results in a spread of frequency: $h * \Delta \nu = \Delta E$, which then gives a relation between the lifetime of a state and the frequency spread [8].

$$h\Delta t\Delta\nu \geq \frac{h}{4\pi} \qquad \textit{eq 3}$$

$$\Delta\nu \geq \frac{1}{4\pi\Delta t} \qquad \textit{eq 4}$$

Ignoring any other factors or conditions, this is the most resolute a line can be. In the terahertz region of the spectrum for rotational spectroscopy, which is the specific region we are studying, the natural linewidth is typically less than 1 Hz, and is too narrow to observe.

Outside factors and conditions can widen the frequency curve. The widening of the curve is called line broadening. The lines in a spectrum will be less resolute the more they are broadened, which makes the lines more difficult to identify.

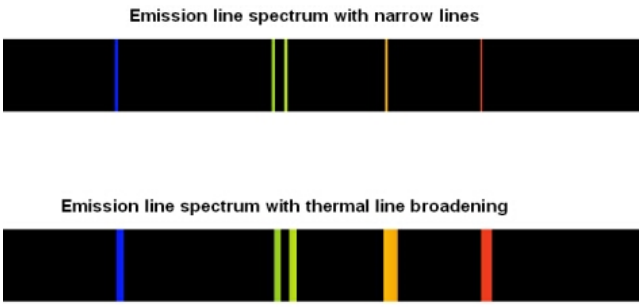

Figure 3: An emission line spectrum with unbroadened lines followed by the same spectrum with broadened lines [13].

There are many sources of line broadening depending on the conditions of the particles used. The two that are discussed in this project are Doppler broadening and pressure broadening.

2.2.2 Doppler Broadening

Doppler Broadening describes when the frequency is shifted due to the Doppler effect. This occurs when molecules move randomly with few molecular interactions. This will be more prevalent in lower pressures, where the density of molecules is low, and collisions are less frequent, giving molecules longer lifetimes.

The line broadening in frequency, $\Delta\nu_D$ due to Doppler broadening from all present velocities can be found using equation 5. The shift in frequency, given in units of Hz, is dependent on the peak frequency, ν_0, also in Hz, the temperature, T, in Kelvin, and mass, M, in atomic mass units [5].

$$\Delta\nu_D = 2\nu_0\sqrt{\frac{2kTln(2)}{mc^2}} = 7.2 * 10^{-7}\nu_0\sqrt{\frac{T}{M}} \qquad \textit{eq 5}$$

Since the Doppler line shift is dependent on both ν_0 and M, it is molecule specific. The Doppler line shift will vary based on the molecule, making Doppler broadening a type of inhomogeneous line shape broadening [5].

Water molecules have one transition frequency at 183 GHz [10]. A water molecule has a mass of 18.02 amu. Looking at example conditions of a temperature of 100 K, the Doppler broadened line width would be 0.31 MHz.

2.2.3 Pressure Broadening

Pressure broadening describes when the frequency shifts due to molecular interactions. This type of broadening is more prevalent in higher pressures and higher densities where the interactions between molecules, typically collisions, limit the lifetime.

The line broadening in frequency, $\Delta\nu_{pb}$ due to pressure broadening can be found using equation 6, where τ is the mean time between collisions that cause changes in energy levels. The shift in frequency is directly proportional to pressure, p.

$$\Delta\nu_{pb} = \frac{1}{2\pi\tau} = bp \qquad \textit{eq 6}$$

Where b is the pressure broadening coefficient. The pressure broadening shift is only dependent on the mean time between collisions, which is dependent on density, which is dependent on pressure. The shift is nearly the same across all peak frequencies and masses, making pressure broadening a type of homogeneous line shape broadening [5].

Using the example of the water molecule from above, we can find the pressure needed to make the pressure broadening equal to the Doppler broadening, as this is the ideal pressure for this type of spectroscopy as it maximizes the depth of absorption and spectral resolution. A typical value for the pressure broadening coefficient is 10 MHz/Torr. Using this, the desired operating pressure should be less than or equal to 31 mTorr. At higher pressures, while the line width broadens, it does not increase in intensity. The spectral line width is constant at lower pressures, and intensity decreases with pressure. Operating at this pressure, 31 mTorr, creates an ideal situation with the greatest spectral resolution and sensitivity.

2.2.4 Interstellar Line Broadening

Molecules in interstellar space are under very extreme conditions. This includes very low temperatures and densities. Temperatures can range from 10 to 100K, with ionized regions having exceptionally high temperatures. Densities in interstellar space can range from 1 to 10^8 cm^{-3}. These low densities make the probability of pressure broadening in interstellar space virtually zero. Doppler broadening is the only type of line broadening that occurs in these conditions [3][6]. When studying molecules in a laboratory, we need to be able to create similar results in terms of line broadening, with minimal pressure broadening and mainly Doppler broadening.

2.3 Vacuum systems

The desired pressure range dictates the types of vacuum pumps in the vacuum system. Based on the previous calculations, our ideal operating pressure is 31 mTorr. A vacuum pump decreases the pressure of a system. This can be achieved in a variety of ways, resulting in different operating pressures.

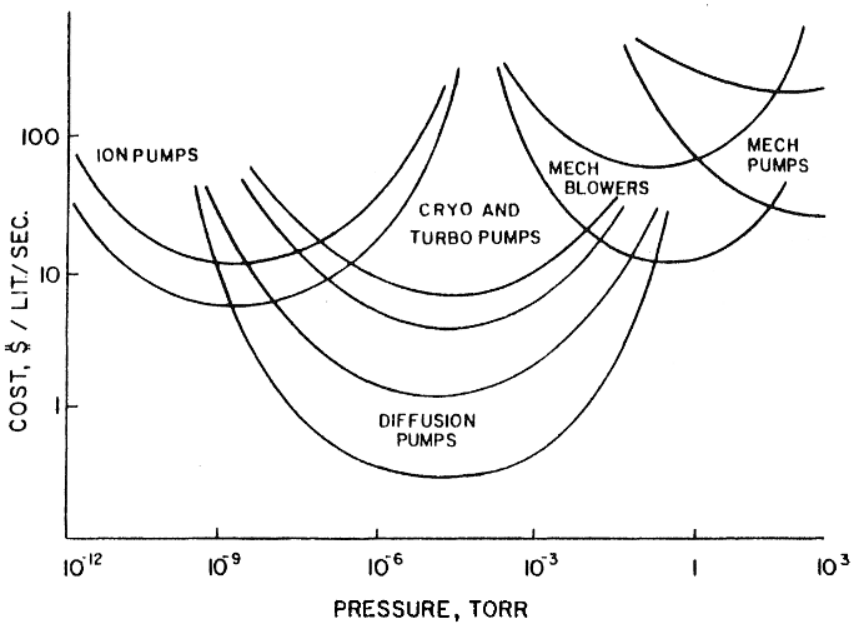

Figure 4: Graph showing the effectiveness and operating pressures of different types of vacuum pumps [9].

Mechanical pumps use mechanical parts to move the gas. This can be achieved using parts like pistons and vanes. Most mechanical pumps used use either rotary vanes or rotary pistons. Both types have specific chambers with moving parts. As the parts move, gas fills the empty chamber via the input. The parts then move the gas to the exhaust, leaving the pump. In our tests, a rotary vane pump was used.

Mechanical pumps have a higher operating pressure range. This will bring the system to a rough vacuum, defined as greater than 10^{-2} Torr [9], and thus are also known as roughing pumps. This is insufficient to reach our operating pressure, to evacuate the cell, and to remove the sample gas.

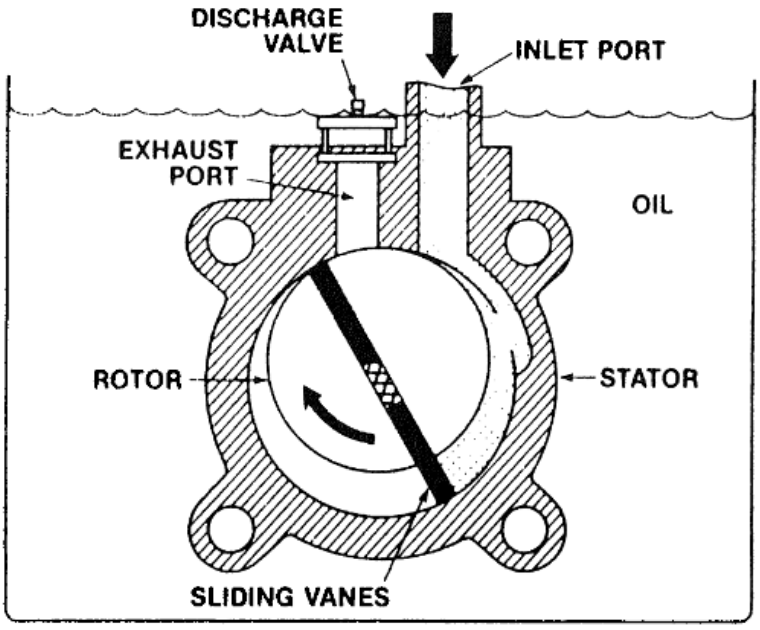

Figure 5: Cross-sectional diagram of a Rotary Vane pump [9].

Diffusion pumps use momentum transfer to move gas. These can achieve much lower pressures than the mechanical pumps. A diffusion pump, also known as a vapor jet pump, is made of a chamber with oil. As the oil heats up, it moves to the exit. Gas from the system will gain momentum from the moving oil and will exit. The oil chamber is made so that once the gas exits the pump, the oil will return to the initial point and restart the process. Diffusion pumps can only operate in a system after a mechanical pump to bring the pressure down to the proper functioning pressure. Diffusion pumps can reach pressures of 10^{-6} Torr. At this pressure and density in a laboratory absorption cell, the absorption spectrum would be too weak to observe, and this would be considered an evacuated cell where the gas sample is removed.

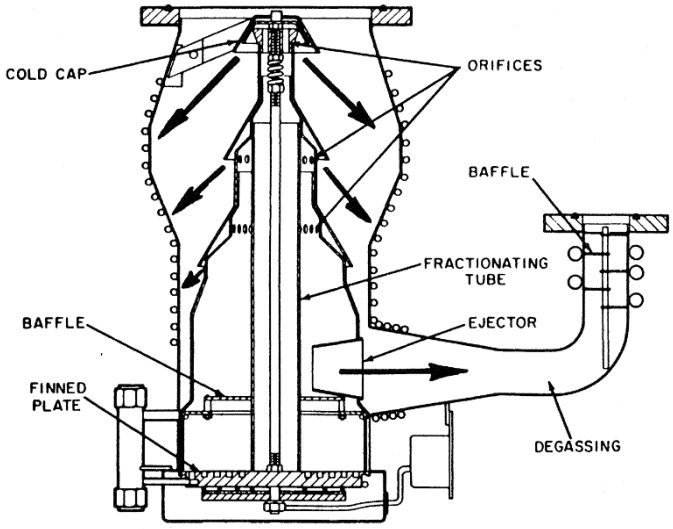

Figure 6: Cross-sectional diagram of a Diffusion pump [9].

Capacitance manometers are tools used to measure pressure. The manometer produces a voltage linearly proportional to the measured pressure. A cross-sectional diagram is shown in figure 7. When connected to the vacuum system, the manometer's metal diaphragm will contort, which affects the circuit inside the manometer. The change in capacitance due to the diaphragm movement results in a voltage linearly proportional to the pressure of the system [2].

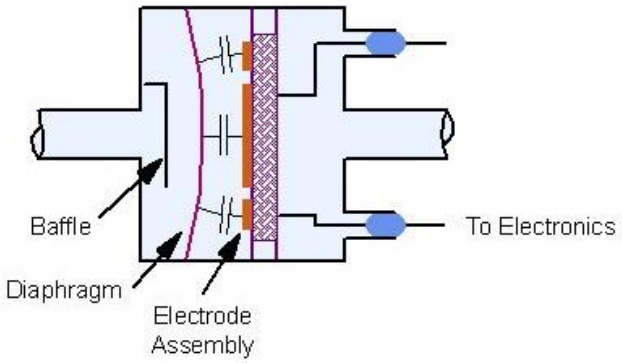

Figure 7: Cross-sectional diagram of a capacitance manometer [2].

3 Methodology

The goal of this project is to model and locate the leakage in the system.

3.1 System

The system consists of a mechanical roughing pump, a diffusion pump, and an absorption cell. The absorption cell, where the sample is studied, is 10.16 cm in diameter and has a length of 1.7 m. It is made of five glass tubes with metal clamps holding them together and gaskets to seal the vacuum. Each end is sealed with Teflon windows and rubber gaskets. The sample enters the cell at the right end of the cell, and a detector is on the left side.

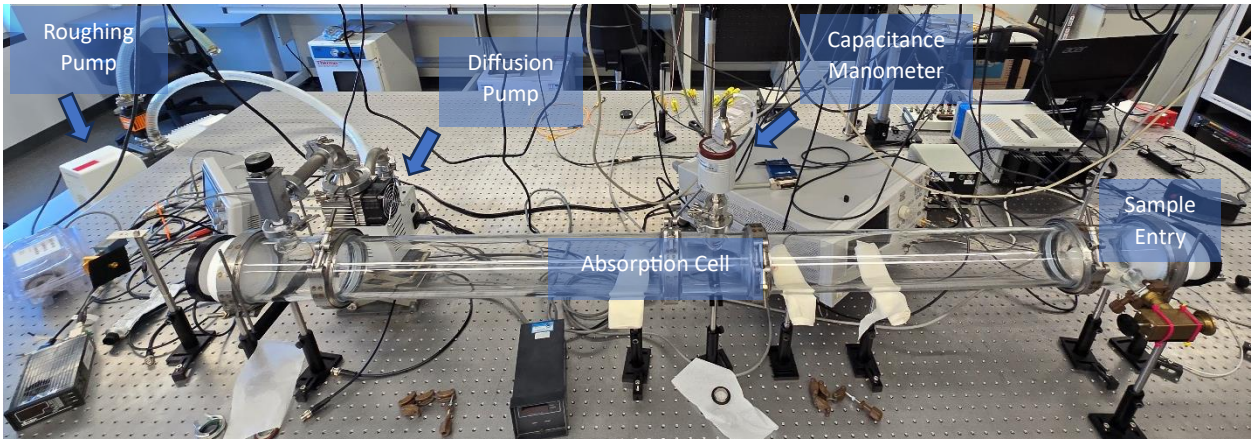

Figure 8: Image of the full system.

Two vacuum pumps are used in this system, a diffusion pump, and a roughing pump. Diffusion pumps can only operate at an inlet pressure in the order of 100 mTorr. Because of this, the diffusion pump can only be turned on after the roughing pump.

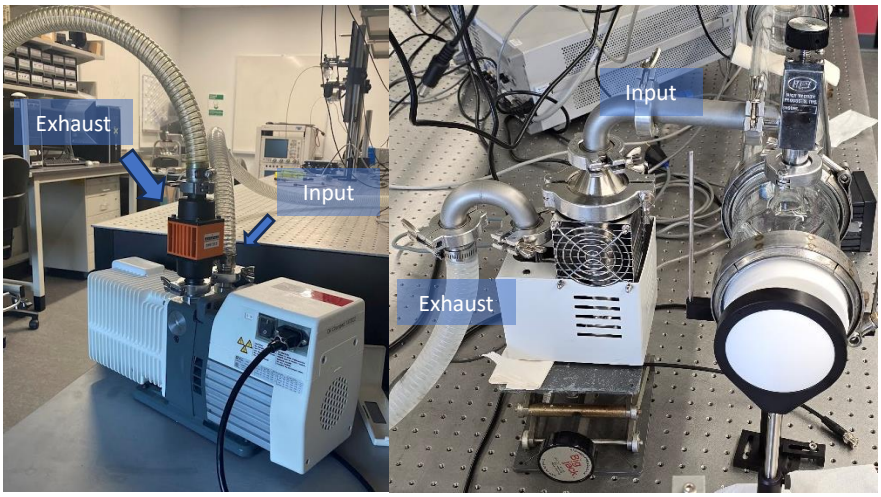

Figure 9: Side-by-side pictures of the roughing pump (left) and diffusion pump (right). Both have the input and exhaust labeled. While pumping down, gas will move from the input to the exhaust.

The roughing pump used in this system is an Adixen 2021SD rotary vane pump from Pfieffer Vacuum. This two-stage rotary vane pump has a pumping speed of 22 m^3/hr, or 0.0061 m^3/s and an ultimate vacuum pressure of 7.5 mTorr. The diffusion pump used in this system is a Welch ProBoost model 1392 air-cooled diffusion pump. This diffusion pump has a pumping speed of 80 L/s, or 0.08 m^3/s. The ultimate vacuum pressure for the diffusion pump is 0.02 mTorr and a maximum discharge pressure of 0.2 Torr. This pump has a volume of $3.6 \pm 0.4 * 10^{-4}$ m^3. Between the two pumps is a connecting tube with a diameter of 0.0254 m and is 2.13 m long, resulting in a volume of $1.08 \pm 0.1 * 10^{-3}$ m^3.

3.2 Software

All data was collected using Vernier Graphical Analysis, with a Vernier Go Direct Voltage Probe and a capacitance manometer. The capacitance manometer was connected to the

specific system component to be looked at. The voltage probe was connected to the capacitance manometer. Two capacitance manometers were used, one that had a maximum pressure of 1000 Torr, and one that had a maximum pressure of 1 Torr. The capacitance manometers used are 626D Unheated Absolute Baratron Capacitance Manometers. Mainly the 1 Torr manometer was used. The capacitance manometer produced a voltage on the scale of 1 Torr to 10 Volts. This capacitance manometer had an upper detection limit of 1 Torr with an accuracy of 25%, so 1 ± 0.25 Torr. All data was collected with a rate of 60 Hz.

3.3 Data Collection

In accordance with the goal to model the system, pressure was monitored both to atmosphere and to vacuum. In all tests, only the roughing pump was turned on.

Vacuum to atmospheric pressure was used to get a basic understanding of the pumps and vacuum system. For this test, the capacitance manometer was connected to the input of the roughing pump. While data was being collected, the roughing pump was turned on, pumping the system down to a rough vacuum until the pressure leveled. Then, while continuing to collect data, the roughing pump was turned off. Data collected stopped when the pressure reached the manometer's limit. This was done three times.

Pressure when going from atmospheric pressure to vacuum was collected and was able to be modeled. For this, the manometer was connected to the input of the system and while data collection was running, the roughing pump was turned on. This was done in three different configurations. First, only the roughing pump was included in the system, with the manometer

connected to the input. Then the roughing pump and the diffusion pump were connected by a tube, and the manometer was connected to the input of the diffusion pump. Finally, the roughing pump, diffusion pump, and absorption cell were all connected, and the manometer was attached to the cell as seen in figure 8. For all trials from atmospheric pressure to vacuum, data collection started then the roughing pump was turned on. Data collection ran until the pressure was stable.

When decreasing pressure with a vacuum pump, assuming the pumping speed of said pump is constant, the pressure can be modeled using equation 7.

$$P(t) = P_{UV} + P_0 e^{\frac{-t}{\tau}} \qquad \textit{eq 7}$$

Pressure over time, $P(t)$, is dependent on the original pressure, P_0, and the characteristic time, τ, and can reach an ultimate vacuum, P_{UV}, depending on the type of pump. The ultimate pressure for each type of pump is shown in figure 4. The characteristic time is given by,

$$\tau = \frac{V}{S} \qquad \textit{eq 8}$$

and depends on the volume of the system, V, over the pump-down speed, S. Here, S is assumed to be constant.

4 Results

4.1 Vacuum to Atmospheric Pressure

The data collected when the pump is going from a rough vacuum to atmospheric pressure will be analyzed qualitatively. These tests were performed to get a basic understanding of the behavior of the pumps in the system and to recognize the presence of leaks in the vacuum system. Initial tests measured the roughing pump. While the data collection was on, the rough pump was turned on, pumped down to a rough vacuum, then turned off and data collection continued until the pressure was back to atmospheric pressure. The capacitance manometer detected up to 1.25 torr, which translates to 12.5 volts. Because the manometer did not detect higher than 1.25 torr, the cut off for atmospheric pressure was 1.25 torr.

The initial roughing pump test was done three times, with a few minutes in between each test to allow pressure to fully go to atmospheric. Figure 10 shows that in each test, the pressure increase rate after the pump was turned off was different. Interestingly, the amount of time that the pressure stayed at was relatively inversely proportional to the rate of pressure increase.

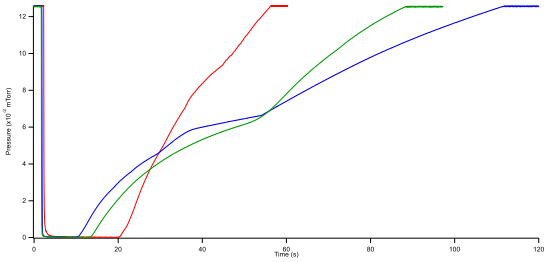

Figure 10: Pressure vs Time graph of all three tests on the roughing pump. The red line represents the data from the first test, the blue line is the second test, and the green line is the third and final test.

The first test, represented in figure 10 by the red line, spent around 16 seconds at the lowest ultimate pressure level. This test took around 36 seconds to increase to the detector limit. The second test, represented in figure 10 by the blue line, spent around 7 seconds at the level pressure and took around 101 seconds to reach the detector limit. The third test, the green line, spent around 10 seconds at level pressure and took around 75 seconds to reach the detector limit. Interestingly, the amount of time left at level pressure inversely affected the pumping up rate. The first test spent the longest time at the ultimate pressure level but took the quickest to increase to the detector limit. The opposite can be said about the second test.

Looking only at the section of the data where the pressure goes from vacuum to atmospheric pressure, the pump-up rate for each test can be compared easily, as seen in figure 11. Each test also had sections where the pump-up rate was not constant. For example, the blue

line has a section from around x=1500 to x=2750 where the pump-up rate decreases and does not show a clean line.

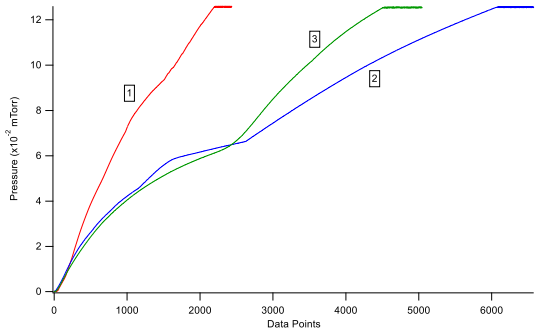

Figure 11: Graph of pressure vs data points showing the sections of each test where the roughing pump was turned off and the pressure was left to return to atmospheric pressure. Each line is labeled in order of tests done. The data acquisition rate was 60 Hz.

4.2 Atmospheric Pressure to Vacuum

While vacuum to atmospheric pressure is useful for qualitative analysis, atmospheric pressure to vacuum can be modeled easily.

In each subsequent test, the volume of the system increased. As the same pump was turned on for all tests, we can assume that the pumping speed is the same in all three tests. It is expected that as the volume increases, the characteristic time increases. Additionally, the time

the system takes to go to the stable ultimate vacuum pressure should increase. The stable ultimate vacuum pressure should increase by a small amount for each test as volume increases.

The test including only the roughing pump was a very quick test. This took less than 1 second to reach the ultimate vacuum pressure. The capacitance manometer was connected directly to the input of the roughing pump, so the volume being evacuated was very small. This pressure was around 3 ± 1 mTorr. The volume of this system only includes the volume of the roughing pump, and the characteristic time is correspondingly small. Given that this is only the roughing pump, everything was as expected.

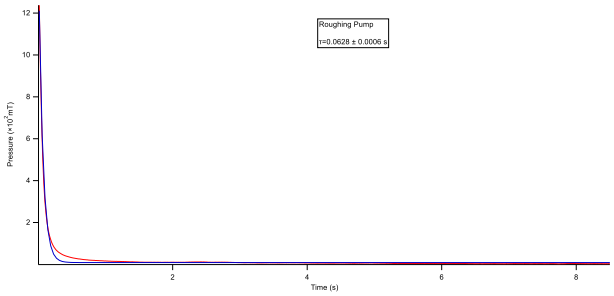

Figure 12: Graph of Pressure vs time of just the roughing pump pump-down. Red is the raw data, blue is the fit data, fit to equation 7. The characteristic time is 0.0628 ± 0.0006 seconds.

The test including the roughing pump and diffusion pump was slightly longer. This took around 25 seconds to reach the level pressure. This level pressure was around 13 ±1 mTorr. The volume of this system includes the volume of the roughing pump, the volume of the diffusion

pump, and the volume of the tube connecting the two. The characteristic time is larger than in the first test by a factor of 28.3436. These factors also describe the difference in volume, as the pumping speed did not change.

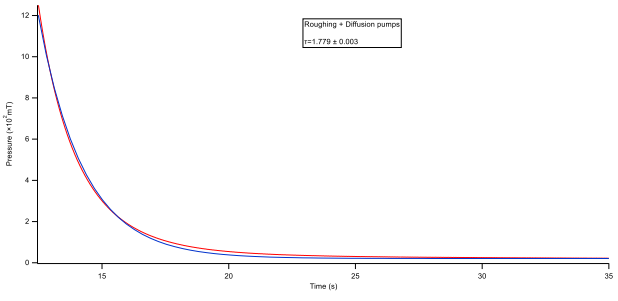

Figure 13: Graph of Pressure vs time of roughing pump and diffusion pump system pump-down. Red is the raw data, blue is the fit data, fit to equation 7. The characteristic time is 1.779 ± 0.003 seconds.

The test of the full system was significantly longer than the other tests. This took around 100 seconds to reach the ultimate vacuum pressure. This ultimate pressure was around 292 ±1 mTorr, much higher than the previous tests. The volume of this system includes the volume of the roughing pump, the volume of the diffusion pump, the volume of the tube connecting the two, and the volume of the entire absorption cell. The characteristic time is larger than the second test by a factor of 9.6 and is larger than the first test by a factor of 271. These factors describe the difference in volume, meaning that the absorption cell added an additional volume 9.6 times the volume of the pumps and connecting tube. The volume of the

absorption cell can be estimated to be 0.0135 m^3. Using this volume and the differences in characteristic times, the volume of the diffusion pump and the connecting tube is around 0.00155 m^3. This is very close to the volume of these two parts as calculated previously, which is $0.00144 \pm 0.00014\ m^3$. This increase in characteristic time was to be expected, but what was not expected was the ultimate vacuum pressure being so high. This test's ultimate pressure was expected to be only slightly higher than the ultimate pressure of the two previous tests, and needs to be closer to the target pressure, 31 mTorr. This proves that the leak is within the cell.

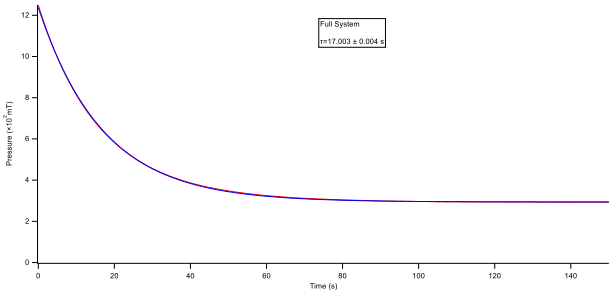

Figure 14: Graph of Pressure vs time of the full system pump-down. Red is the raw data, blue is the fit data, fit to equation 7. The characteristic time is 17.003 ± 0.004 seconds.

5 Conclusions

The goal of this project was to model the system and locate the leak. Throughout this project I realized that in terms of achieving a desired pressure with this system, the general set up of the system makes leaks very probable, especially after continued use.

For all three trials looking at atmospheric pressure to vacuum pressure resulted in the expected characteristic times. As the volume increased, the characteristic time increased, which showed that the pump was working correctly. The first two trials, the trial including just the roughing pump and the trial including the roughing pump, diffusion pump, and the connecting tube, resulted in the expected ultimate lowest pressures, so we can conclude that there are no abnormalities in these two pumps and connecting tube. The only logical location for the leak would be within the absorption cell. The pump-down graph of the whole system verifies this assumption, as the ultimate vacuum pressure was significantly higher than the expected pressure.

The tests described in this project only include the roughing pump running. For all tests, the diffusion pump was not turned on. A full system test with both pumps running was attempted but had to be stopped. After turning both pumps on, a slight hissing sound was detected around the absorption cell. At this point, testing stopped, both pumps were turned off, but the seal was not broken. This made it easier to locate the source of the hissing sound. This was determined to be one of the metal clamps holding the glass tubes together.

In general, the way the cell is built means that there are many possible places for leaks. Each clamp and tube section are their own parts that could move slightly out of place. The stress on the glass tube due to the vacuum can misalign it with the clamps and the rest of the cell, leading to further stress and leaks.

5.1 Recommendations for future work

Given the set-up is not ideal in terms of leak prevention, it would be best for future projects to look at different designs and set ups for absorption spectroscopy cells. At the very least, the cell should be taken apart and put back together again with extra attention to the alignment of the tubes. I also think it would be best for slightly different support locations, especially when building, to make sure the alignments are correct.

6 References

(1) *Absorption and Emission Spectra of Various Elements*. (n.d.). Webb. Retrieved May 13, 2024, from https://webbtelescope.org/contents/media/images/01F8GF9E8WXYS168WRPPK9YHEY

(2) *Baratron Capacitance Manometers*. (n.d.). Retrieved May 14, 2024, from https://www.mks.com/n/baratron-capacitance-manometers

(3) Basu, S., & Sharma, P. (2021). *Essential Astrophysics: Interstellar Medium to Stellar Remnants* (1st ed.). CRC Press. https://doi.org/10.1201/9781003215943

(4) Baxter, J. B., & Guglietta, G. W. (2011). Terahertz Spectroscopy. *Analytical Chemistry*, *83*(12), 4342–4368. https://doi.org/10.1021/ac200907z

(5) Bernath, P. F. *(2020). Spectra of atoms and molecules.* Oxford University Press,. (n.d.).

(6) Carraro, G. (2021). *Astrophysics of the Interstellar Medium*. Springer International Publishing. https://doi.org/10.1007/978-3-030-75293-4

(7) Doppler broadening. (2024). In *Wikipedia*. https://en.wikipedia.org/w/index.php?title=Doppler_broadening&oldid=1218802120

(8) Gordy, W., & Cook, R. L. *(Robert L. (1984).* Microwave molecular spectra (3rd ed. (n.d.).

(9) Hablanian, M. H. (2017). *High-Vacuum Technology: A Practical Guide, Second Edition* (2nd ed.). Routledge. https://doi.org/10.1201/9780203751923

(10) Koshelev, M. A., Vilkov, I. N., Makarov, D. S., Tretyakov, M. Yu., Vispoel, B., Gamache, R. R., Cimini, D., Romano, F., & Rosenkranz, P. W. (2021). Water vapor line profile at 183-GHz: Temperature dependence of broadening, shifting, and speed-dependent shape parameters. *Journal of Quantitative Spectroscopy and Radiative Transfer*, *262*, 107472. https://doi.org/10.1016/j.jqsrt.2020.107472

(11) Kunze, H.-J. (2009). *Introduction to Plasma Spectroscopy* (Vol. 56). Springer Berlin Heidelberg. https://doi.org/10.1007/978-3-642-02233-3

(12) Puzzarini, C., Alessandrini, S., Bizzocchi, L., & Melosso, M. (2023). Hunting for interstellar molecules: rotational spectra of reactive species. *Faraday Discussions*, *245*, 309–326. https://doi.org/10.1039/D3FD00052D

(13) *Thermal Doppler Broadening | COSMOS*. (n.d.). Retrieved May 24, 2024, from https://astronomy.swin.edu.au/cosmos/t/Thermal+Doppler+Broadening

6.1 Machine Manuals

1. Roughing pump-Adixen 2021SD from Pfeiffer Vacuum
2. Diffusion pump-Welch ProBoost model 1392 air-cooled diffusion pump
3. Capacitance Manometers-626D Unheated Absolute Baratron Capacitance Manometers